Indonesian Journal of Earth Sciences, Vol. 2, No. 2 (2022): 157-176

P-ISSN: 2798-1134 | E-ISSN: 2797-3549 | DOI: 10.52562/injoes.v2i2.428

Indonesian Journal of Earth Sciences

http://journal.moripublishing.com/index.php/injoes

Satellite Oceanographic Data Processing and Analysis: Correlation Between Nino 3.4 Sea Surface Temperature & Sea Surface High and Wind

Jen-Yang Lin[1], Ming-Chung Tang[2], Febrianto Wijaya[3]

[1]Department of Oceanography, National Sun Yat-sen University, Kaohsiung, Taiwan
[2]Department of Marine Environmental Informatics, National Taiwan Ocean University, Keelung, Taiwan
[3]Graduate Institute of Hydrological & Oceanic Sciences, National central University, Taoyuan, Taiwan
Correspondence: linjy@nsysu.edu.tw

Received: 08 November 2022; Accepted: 23 December 2022; Published: 26 December 2022

Abstract: El Nino Southern Oscillation (ENSO) is an irregular climate oscillation induced by sea surface temperature anomalies (SSTA) in the Equatorial Pacific Ocean. An anomalous warming in this area is known as El Nino, while an anomalous cooling bears the name of La Nina. The objectives of this study are to: reproduce Oceanic Nino Index (ONI) based on MW OISST; produce Nino Region 3.4 wind and Sea Surface High (SSH); analyze the correlation between SST and Wind & SSH; discuss Typhoon Soudelor based on SST, Wind, and SSH; and analyze the correlation of El Nino and Precipitation in specific area. MWOI-SST was used to produce monthly mean SST over Nino 3.4 region from January 1998 – May 2020. Monthly wind data was obtained from QuickScat. Daily Sea Surface High (SSH) was obtained from Copernicus Marine Environment Monitoring Service (CMEMS). Daily precipitation from TRMM 3B42 over Bandung City (Indonesia) was used to assess the correlation between El Nino and precipitation in specific area. The results show that in Nino 3.4 region, 2015 is the hottest year during 1998-2020 period with average SST of 28.5oC, and 1999 is the coldest year with average SST of 25.7oC. The result shows that the MWOI-SST Ocean Nino Index has very strong correlation with ERSST.v5 with coefficient of correlation is 0.92 and RMSE is 0.36oC. the wind speed of Nino 3.4 region is range from 5.23 m/s to 7.97 m/s. Unlike Sea Surface Temperature (SST), annual average wind speed is more stable with monthly variation. The wind speed is observed high in the beginning and the end of years. Sea Surface Height (SSH) over Nino 3.4 region varied from 65.8 cm to 106.8 cm. 2015 is the highest SSH with annual average of 96 cm, whereas 1999 is the lowest SSH with annual average of 71.4 cm. It is observed that Sea Surface Temperature (SST) has negative correlation with wind speed with coefficient of correlation of 0.28. Conversely, Sea Surface Temperature (SST) over Nino 3.4 region has positive correlation with Sea Surface High (SSH) with coefficient of correlation of 0.30. which mean the higher temperature, the higher Sea Surface Height. During the passage of Typhoon Soudelor, there is evident cool trail along its track with rightward bias. We can assume that the decreasing precipitation in Bandung City might be affected by strong El Nino occurrence in 2015.

Keywords: ENSO, Nino 3.4, SST, SSH, Wind

INTRODUCTION

El Nino Southern Oscillation (ENSO) is a complex climate phenomenon that occurs in the tropical Pacific Ocean and has a significant impact on global weather patterns. An anomalous warming in this area is known as El Nino, while an anomalous cooling bears the name of La Nina (Wang et al., 2018). ENSO is characterized by periodic variations in sea surface temperatures, atmospheric pressure, and wind patterns, which can lead to changes in global climate patterns. These changes can affect temperature, precipitation, and storm patterns, and can have significant impacts on agriculture, water resources, and human health (Kovats, 2000). ENSO is well recognized as the dominant mode of interannual variability in the Pacific Ocean and it affects the atmospheric

general circulation which transmits the ENSO signal to other parts of world (Deliège &Nicolay, 2017). El Nino recurs at some time between 2 and 7 years, or 4.5 years on average, and can last from 9 to 18 months. From 1950 to 2020, 23 El Nino episodes officially occurred using the ONI threshold criterion (Glantz & Ramirez, 2020).

According to Banholzer & Donner (2014) and Hayashi et al. (2020), ENSO is driven by the interaction between the ocean and the atmosphere in the tropical Pacific, and is characterized by three phases: El Nino, La Nina, and Neutral. During an El Nino event, the eastern Pacific Ocean warms, leading to an increase in atmospheric pressure and a decrease in wind strength. This can result in a shift in global weather patterns, including an increase in rainfall in some regions and a decrease in others. In contrast, during a La Nina event, the eastern Pacific Ocean cools, leading to a decrease in atmospheric pressure and an increase in wind strength. This can also result in a shift in global weather patterns, including an increase in drought conditions in some regions and an increase in flooding in others.

ENSO events can have significant impacts on global climate patterns, including the monsoon season in Asia and the hurricane season in the Atlantic (Wu, et al., 2009). Research has also shown that ENSO can affect agricultural production, water resources, and human health. For example, drought conditions associated with El Nino events can lead to crop failures and food shortages, while heavy rainfall and flooding associated with La Nina events can lead to water contamination and the spread of disease (Jorgensen, 2016). ENSO values can be demonstrated by the Oceanic Nino Index (ONI) as well as changes in sea surface temperature that have an impact on rainfall intensity. The Oceanic Niño Index (ONI) has become the de-facto standard that NOAA uses for identifying El Niño (warm) and La Niña (cool) events in the tropical Pacific (Prasetyo & Nabilah, 2017).

The Ocean Nino Index (ONI) is a measure of the sea surface temperature (SST) anomaly in the central and eastern tropical Pacific Ocean. It is used to monitor and classify El Niño and La Niña events, which are large-scale climate patterns that can have significant impacts on weather patterns, agriculture, and other aspects of the Earth's climate system (Rodríguez-Morata et al., 2019). El Niño events are characterized by warmer-than-normal SSTs in the tropical Pacific, while La Niña events are characterized by cooler-than-normal SSTs. The ONI is calculated based on the three-month running mean of the SST anomaly in the region between 5°N and 5°S, and 170°W and 120°W (Shabbar, 2006) (Figure 1). According to the National Oceanic and Atmospheric Administration (NOAA, 2022), El Niño events are declared when the ONI is greater than or equal to 0.5°C for at least five consecutive months, while La Niña events are declared when the ONI is less than or equal to -0.5°C for at least five consecutive months.

The temperature of the upper layer of the ocean, referred to as sea surface temperature (SST), plays a significant role in determining the climate and weather patterns of a specific region, as well as influencing the behavior and distribution of marine life (Hartmann, 2015). On the other hand, wind, which is the movement of air over the Earth's surface, is caused by variations in temperature and pressure and plays a crucial role in the transfer of heat and moisture between the Earth's surface and the atmosphere (Nachshon et al., 2012). Additionally, sea surface height (SSH), which refers to the height of the ocean's surface in relation to a reference point, is impacted by various factors such as the water's temperature and salinity, the density of the water, and the gravitational forces of the Earth and Moon (Zhuang et al., 2010).

There is a strong correlation between SST and wind, as well as between SST and SSH. A study by Philander (1989) found that the El Niño-Southern Oscillation (ENSO) cycle has a strong influence on global wind and SST patterns in the tropical Pacific Ocean. Li & Han (2015) also found that wind speed and direction can significantly impact SST through surface heat exchange, particularly in regions with strong and persistent winds. Additionally, Church & White (2006) discovered that the thermal expansion effect, the relationship between SST and sea surface height, plays a major role in observed sea level rise over the past century due to increasing SST caused by global warming. Changes in SST can affect wind patterns and the exchange of heat and moisture between the ocean and the atmosphere, which in turn can influence the height of the ocean surface.

Similarly, changes in wind patterns and SSH can affect SST by influencing the exchange of heat and moisture between the ocean and the atmosphere. All of these factors are interconnected and can influence one another in complex ways, making it difficult to predict how they will behave in the future.

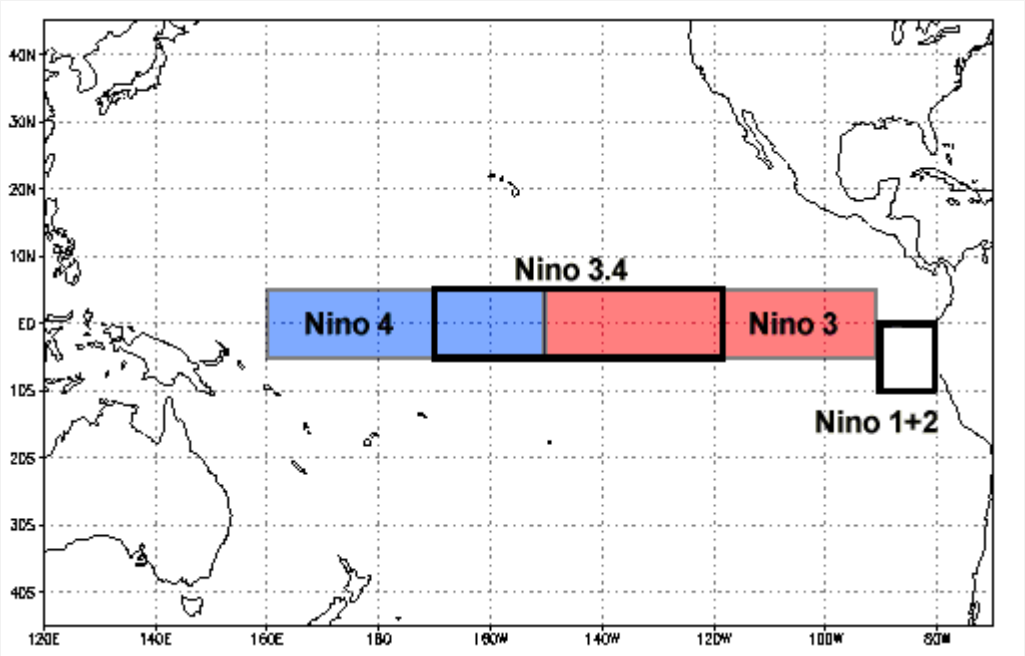

Figure 1. Niño Regions

This study aims to reproduce the ONI using the MW OISST data, which is a dataset of global SST observations from satellite and in situ measurements. In addition to this, the study aims to produce Nino Region 3.4 Wind and Nino Region 3.4 Sea Surface High data, which will provide further information on the atmospheric and oceanic conditions in the tropical Pacific region. We will then analyze the correlation between the SST and Wind & SSH data in order to understand how these variables are related to each other and how they may affect the ONI. In the final stages of the study, we will discuss Typhoon Soudelor, a tropical cyclone that affected the Pacific region in 2015, based on the SST, Wind, and SSH data. Finally, the study will also analyze the correlation between El Nino and precipitation in a specific area, in order to understand how these two variables are related and how they may affect the weather patterns in that region.

DATA & METHOD

The Daily Microwave Optimally Interpolated Sea Surface Temperature (MWOI-SST) is a method for producing high-resolution, daily Sea Surface Temperature (SST) estimates using microwave satellite data. It has been widely used in climate research and has been shown to be a reliable source of SST data. The MWOI-SST method begins by collecting microwave satellite data from sensors on satellites orbiting the Earth. These sensors measure the microwave emissions from the Earth's surface, which are sensitive to the temperature of the surface water. The satellite data is combined with in situ measurements of SST taken from ships, buoys, and other sources to produce a gridded, daily estimate of SST. The MWOI-SST method has several advantages over other methods of estimating SST. It is able to produce high-resolution, daily SST estimates, even in areas where in situ measurements are scarce. It is also relatively insensitive to atmospheric conditions, such as clouds and precipitation, which can make it difficult to measure SST using other methods.

In this study, the MWOI-SST was used to calculate the monthly mean SST over the Nino 3.4 region, which is a region in the tropical Pacific Ocean that is known to be a key indicator of global climate variability. The monthly mean SST was calculated for the period from January 1998 to May 2020 using geoprocessing techniques and the ArcGIS Model Builder software (Figure 2). To obtain the Oceanic Nino Index (ONI), the monthly MWOI-SST data was compared to a 30-year base period and the resulting anomalies were calculated.

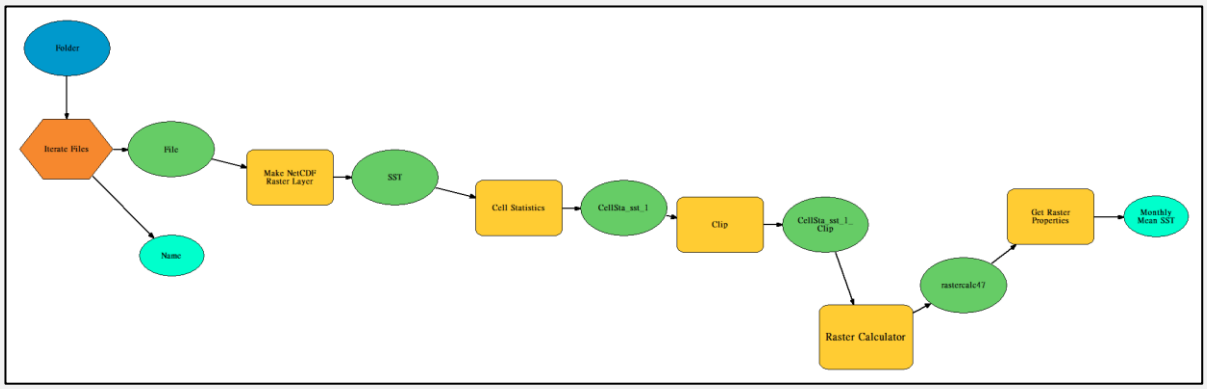

Figure 2. ArcGIS Model Builder framework to produce monthly mean SST

Monthly wind data for the Nino 3.4 region was obtained from the Quick Scatterometer (QuickScat), a satellite instrument launched in June 1999 and operated until November 2009. Using ArcGIS, the monthly wind data was plotted and analyzed. In addition, daily Sea Surface Height (SSH) data was obtained from the Copernicus Marine Environment Monitoring Service (CMEMS), which processes altimeter data from various missions including Jason-3, Sentinel-3A, and others. The data is processed by the SL-TAC multimission altimeter data processing system. To study the correlation between El Nino and precipitation, daily precipitation data from the Tropical Rainfall Measuring Mission (TRMM) 3B42 was also used, specifically for the Bandung City region in Indonesia.

RESULT & DISCUSSION

MWOI-SST Oceanic Nino Index

The MWOI-SST (Multivariate ENSO Index - Standardized Sea Surface Temperature) Oceanic Nino Index is a measure of the strength and duration of El Niño and La Niña events in the tropical Pacific Ocean. The index is based on standardized sea surface temperature (SST) anomalies in the region of the tropical Pacific Ocean known as the Nino 3.4 region, which is defined as the area between 5°S and 5°N and 120°W and 170°W. The MWOI-SST Oceanic Nino Index is used to monitor and predict the impacts of El Niño and La Niña events on global weather patterns and climate.

Sea Surface Temperature (SST) is an essential climate variable for understanding the climate system and quantifying ongoing climatic change. Global mean SST has risen from decade-to-decade since the 1970s, with consequences for global weather patterns and oceanic ecosystems (Merchant et al., 2019). Sea surface temperature anomalies influence the atmosphere by altering the flux of latent and sensible heat from the ocean, and thus providing anomalous heating patterns (Holton & Hakim, 2013). The SST over Nino 3.4 region is essential to analyze the ENSO occurrences. During an El Niño event, the MWOI-SST Oceanic Nino Index tends to be positive, indicating above-normal SSTs in the Nino 3.4 region. During a La Niña event, the MWOI-SST Oceanic Nino Index tends to be negative, indicating below-normal SSTs in the Nino 3.4 region.

The result shows that in Nino 3.4 region, 2015 is the hottest year during 1998-2020 period with average SST of 28.5°C, and 1999 is the coldest year with average SST of 25.7°C. March – June

is the hottest months based on monthly average SST over the region. The following figures and table are the results for monthly SST.

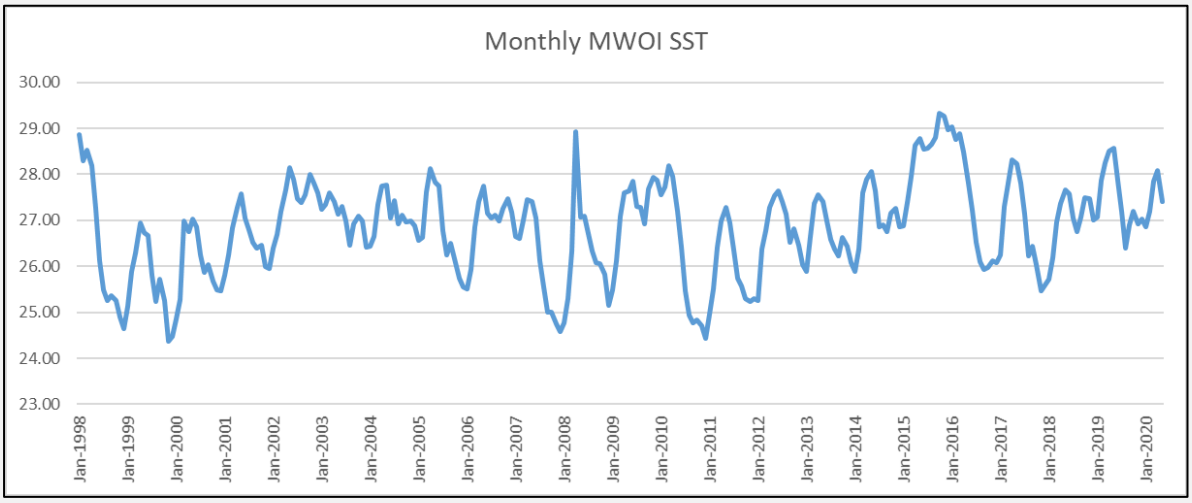

Figure 3. Monthly MWOI-SST timeseries

Table 1. Monthly Sea Surface Temperature (SST) over Nino 3.4 region

	1	2	3	4	5	6	7	8	9	10	11	12
1998	28.9	28.3	28.5	28.2	27.3	26.1	25.5	25.3	25.4	25.3	24.9	24.6
1999	25.1	25.9	26.3	26.9	26.7	26.7	25.8	25.2	25.7	25.3	24.4	24.5
2000	24.8	25.3	27.0	26.8	27.0	26.9	26.2	25.9	26.0	25.7	25.5	25.5
2001	25.8	26.2	26.8	27.3	27.6	27.0	26.8	26.5	26.4	26.5	26.0	25.9
2002	26.4	26.7	27.2	27.7	28.1	27.9	27.5	27.4	27.5	28.0	27.8	27.6
2003	27.2	27.3	27.6	27.4	27.1	27.3	27.0	26.4	26.9	27.1	27.0	26.4
2004	26.4	26.6	27.3	27.8	27.8	27.1	27.4	26.9	27.1	27.0	27.0	26.9
2005	26.6	26.6	27.6	28.1	27.8	27.7	26.8	26.2	26.5	26.2	25.7	25.5
2006	25.5	25.9	26.9	27.4	27.7	27.2	27.0	27.1	27.0	27.3	27.5	27.2
2007	26.7	26.6	27.0	27.5	27.4	27.1	26.1	25.5	25.0	25.0	24.7	24.6
2008	24.8	25.3	26.3	28.9	27.1	27.1	26.7	26.3	26.1	26.1	25.8	25.1
2009	25.5	26.1	27.1	27.6	27.6	27.9	27.3	27.3	26.9	27.7	27.9	27.9
2010	27.6	27.7	28.2	28.0	27.2	26.4	25.5	24.9	24.8	24.8	24.7	24.4
2011	25.0	25.5	26.4	27.0	27.3	26.9	26.4	25.8	25.6	25.3	25.2	25.3
2012	25.2	26.4	26.8	27.3	27.5	27.6	27.4	27.1	26.5	26.8	26.5	26.0
2013	25.9	26.7	27.4	27.6	27.4	27.0	26.6	26.4	26.2	26.6	26.4	26.1
2014	25.9	26.4	27.6	27.9	28.1	27.6	26.8	26.9	26.8	27.1	27.3	26.9
2015	26.9	27.4	28.0	28.6	28.8	28.5	28.6	28.7	28.8	29.3	29.3	29.0
2016	29.0	28.8	28.9	28.5	27.8	27.2	26.5	26.1	25.9	26.0	26.1	26.1
2017	26.3	27.3	27.8	28.3	28.2	27.8	27.1	26.2	26.4	26.0	25.5	25.6
2018	25.7	26.2	27.0	27.4	27.7	27.6	27.1	26.7	27.1	27.5	27.5	27.0
2019	27.1	27.9	28.2	28.5	28.6	27.9	27.2	26.4	26.9	27.2	26.9	27.0
2020	26.9	27.2	27.9	28.1	27.4							

Based on the Figures 3, 4, and 5, and Table 1, it appears that the average SST in the Nino 3.4 region was highest in 2015, with an average temperature of 28.5°C. This is likely due to the presence of an El Niño event during that year, which can lead to warmer-than-average SSTs in the region. On the other hand, the coldest year on record was 1999, with an average SST of 25.7°C.

This could be due to the presence of a La Niña event, which is associated with cooler-than-average SSTs in the Nino 3.4 region.

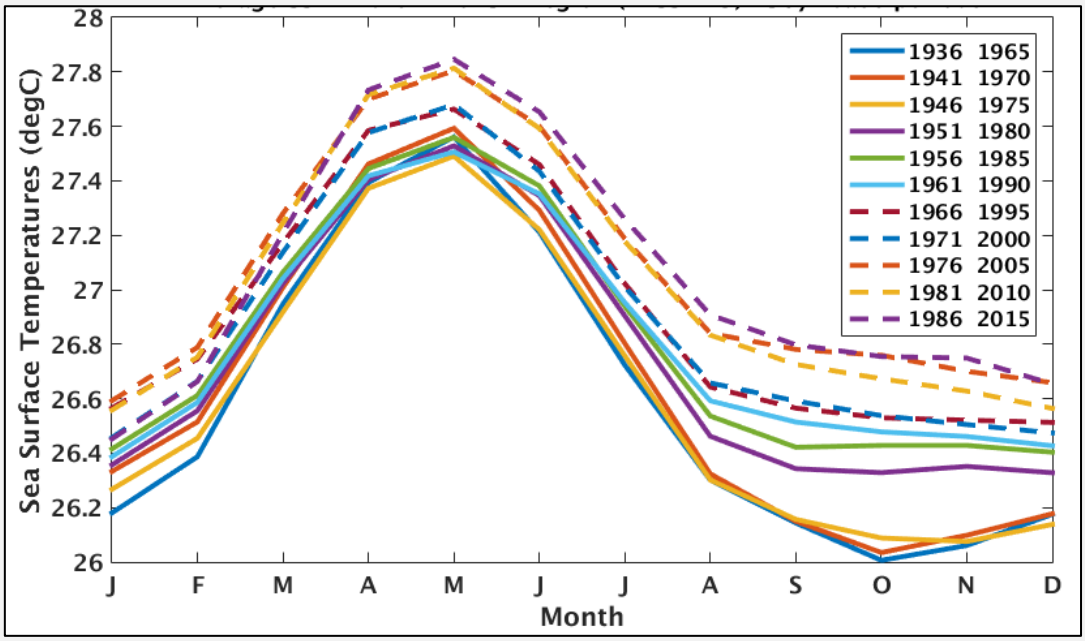

Figure 4. Average SST in the Nino 3.4 region (ERSST.v5)- 30yr base periods

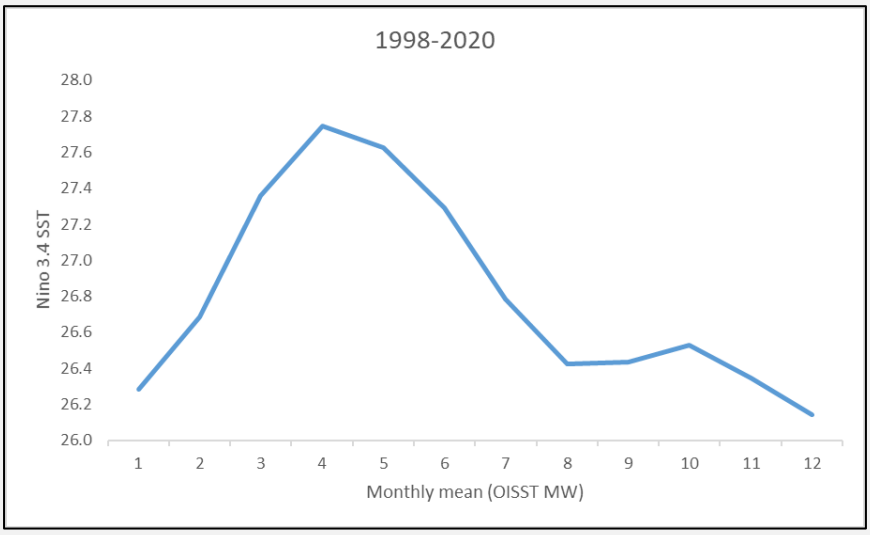

Figure 5. Average SST in Nino 3.4 region (MWOI-SST)

The months of March through June are typically the hottest in the Nino 3.4 region, based on the monthly average SSTs. This is likely due to the fact that these months fall within the Northern Hemisphere's spring and summer seasons, and the Nino 3.4 region is located in the tropics, where temperatures are relatively warm year-round.

It's important to note that ENSO events can have a significant impact on global weather patterns, and they can lead to fluctuations in temperature and precipitation levels in various regions around the world. Understanding the characteristics of ENSO and its impacts on the climate can be

important for a variety of applications, including agriculture, natural resource management, and emergency preparedness.

Table 2. 3-month running mean of MWOI-SST anomalies in the Niño 3.4 region

Year	DJF	JFM	FMA	MAM	AMJ	MJJ	JJA	JAS	ASO	SON	OND	NDJ
1998	1.9	1.7	1.1	0.4	-0.5	-1.2	-1.6	-1.5	-1.4	-1.5	-1.7	-1.7
1999	-1.4	-1.1	-0.9	-0.9	-0.9	-1.1	-1.3	-1.3	-1.3	-1.6	-1.9	-2.0
2000	-1.8	-1.1	-0.9	-0.7	-0.8	-0.8	-0.9	-0.9	-0.9	-0.9	-1.1	-1.0
2001	-0.7	-0.5	-0.4	-0.4	-0.4	-0.4	-0.5	-0.4	-0.4	-0.5	-0.6	-0.5
2002	-0.2	0.0	0.0	0.1	0.2	0.3	0.3	0.5	0.8	1.0	1.1	0.9
2003	0.8	0.6	0.2	-0.2	-0.5	-0.5	-0.4	-0.2	0.0	0.2	0.1	0.0
2004	-0.1	0.0	0.0	0.0	-0.2	-0.2	-0.1	0.2	0.2	0.3	0.2	0.2
2005	0.1	0.2	0.3	0.3	0.2	-0.1	-0.4	-0.5	-0.5	-0.6	-0.9	-1.0
2006	-0.9	-0.7	-0.5	-0.3	-0.3	-0.3	-0.2	0.1	0.3	0.5	0.6	0.5
2007	0.2	0.0	-0.2	-0.3	-0.4	-0.7	-1.0	-1.4	-1.6	-1.9	-1.9	-1.9
2008	-1.7	-1.3	-0.3	-0.2	-0.1	-0.6	-0.6	-0.6	-0.7	-0.8	-1.0	-1.1
2009	-1.0	-0.5	-0.3	-0.2	-0.1	0.0	0.2	0.2	0.5	0.7	1.1	1.2
2010	1.1	1.1	0.8	0.2	-0.6	-1.2	-1.7	-1.9	-2.0	-2.0	-2.1	-1.9
2011	-1.6	-1.1	-0.9	-0.7	-0.7	-0.7	-0.9	-1.1	-1.3	-1.4	-1.4	-1.4
2012	-1.0	-0.6	-0.4	-0.4	-0.3	-0.1	0.1	0.0	0.0	-0.2	-0.3	-0.5
2013	-0.4	-0.1	0.0	-0.2	-0.4	-0.6	-0.6	-0.6	-0.4	-0.3	-0.3	-0.5
2014	-0.5	-0.2	0.1	0.2	0.1	-0.1	-0.1	-0.2	0.1	0.3	0.4	0.4
2015	0.5	0.6	0.8	0.9	0.9	1.0	1.3	1.7	2.1	2.4	2.5	2.5
2016	2.3	2.1	1.5	0.8	0.1	-0.4	-0.7	-0.8	-0.8	-0.8	-0.7	-0.5
2017	0.0	0.3	0.6	0.5	0.4	0.1	-0.2	-0.4	-0.6	-0.8	-1.0	-1.0
2018	-0.8	-0.5	-0.4	-0.3	-0.2	-0.2	-0.1	0.0	0.3	0.6	0.6	0.6
2019	0.7	1.0	1.0	0.8	0.6	0.3	-0.1	-0.2	0.0	0.2	0.3	0.3
2020	0.4	0.5	0.5	0.2	0.0	-0.4						

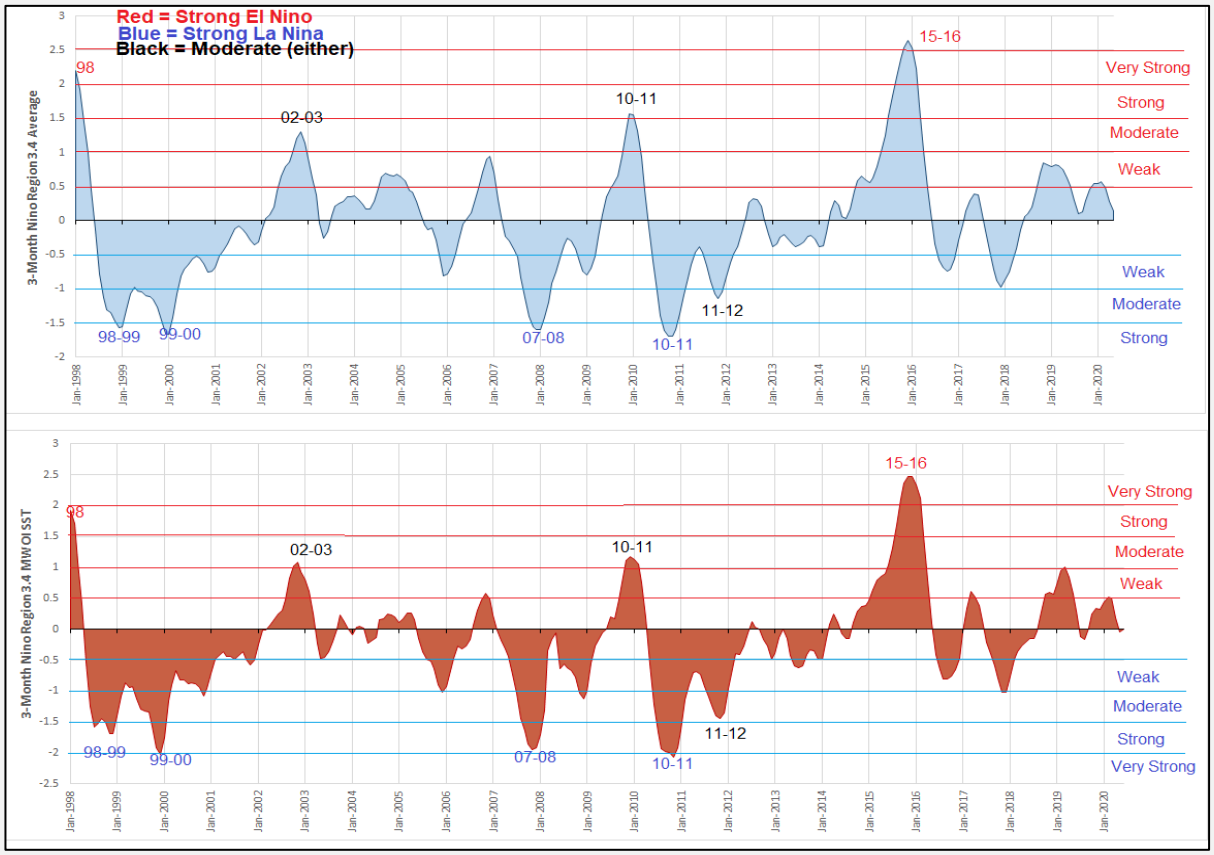

Figure 6. The Comparison of Oceanic Nino Index (ONI) with El Nino and La Nina strength years through the period of study (1998-May 2020)
a). ERSST.v5 Ocean Nino Index, b). MWOI-SST Ocean Nino Index

Based on Table 2 and Figure 6, we can observe that the El Nino occurrences is observed in 1998, 2002-2003, 2010-2011, and 2015-2016 in different categories. With up to 2.5-degree anomaly, year of 2015 categorized as very strong El Nino. The beginning of 1998 also identifies as very strong El Nino category, whereas 2002-2003 and 2009-2010 are identified as moderate El Nino.

For La Nina strength, there are 4 periods identified as strong La Nina including 1998-1999, 1999-2000, 2007-2008, and 2010-2011. the period of 2011-2012 categorize as moderate La Nina. SST values in the Niño 3.4 region may not be the best choice for determining La Niña episodes but, for consistency, the index has been defined by negative anomalies in this area. A better choice might be the Niño 4 region, since that region normally has SSTs at or above the threshold for deep convection throughout the year.

There are two different versions of the ONI: the Extended Reconstructed Sea Surface Temperature version 5 (ERSST.v5) and the Multivariate ENSO Index (MEI) based on the SST data from the Met Office Hadley Centre (MWOI-SST). Both versions use the same definition of the Niño 3.4 region and are based on the same underlying SST data, but they use different methods to calculate the ONI.

The ERSST.v5 ONI is calculated by taking the average of the SST anomalies in the Niño 3.4 region over a period of three months. El Niño events are defined as periods of time when the ONI is greater than or equal to +0.5°C, while La Niña events are defined as periods of time when the ONI is less than or equal to -0.5°C.

The MWOI-SST ONI is calculated using a different method that considers the SST anomalies in the entire tropical Pacific Ocean, as well as the atmospheric pressure and winds in the region. El Niño and La Niña events are also defined using the MWOI-SST ONI, with El Niño events being defined as periods of time when the ONI is greater than or equal to +0.5°C and La Niña events being defined as periods of time when the ONI is less than or equal to -0.5°C.

The comparison between ERSST.v5 and MWOI-SST Ocean Nino Index is needed to evaluate the performance of MWOI-SST. The result shows that the MWOI-SST Ocean Nino Index has very strong correlation with ERSST.v5 with coefficient of correlation is 0.92 and RMSE is 0.36oC (Figure 7).

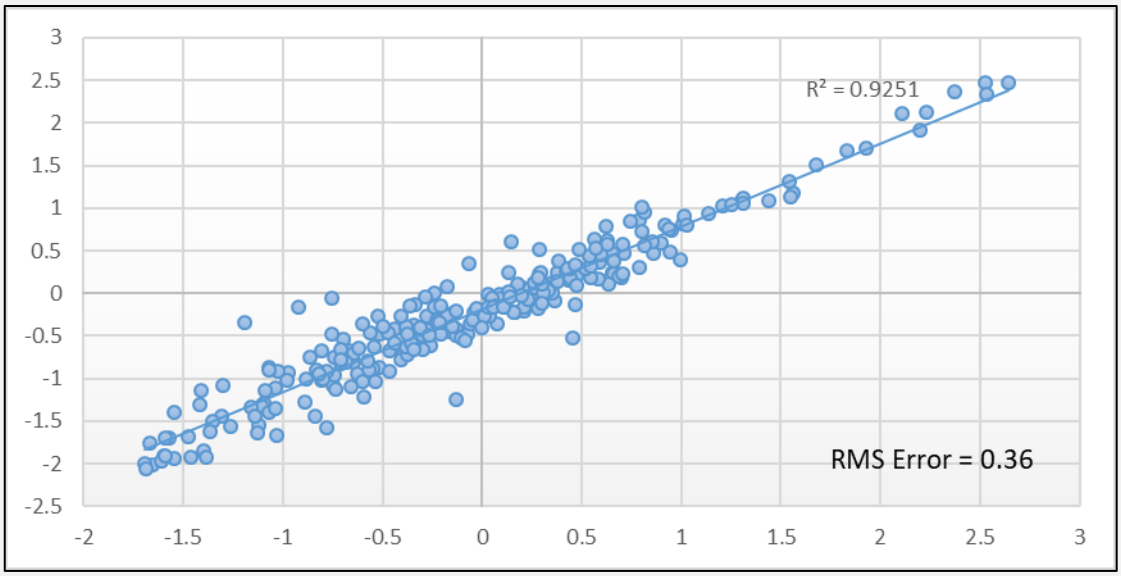

Figure 7. Comparison of ERSST.v5 and MWOI-SST Ocean Nino Index (ONI)

There have been numerous studies that have examined the relationship between the ERSST.v5 and MWOI-SST Oceanic Nino Index (ONI) values. Some of these studies have found a

strong correlation between the two indices. For example, in a study by Lyon & Camargo (2009), the authors compared the ERSST.v3b (a predecessor to ERSST.v5) and MWOI-SST ONI values during the December-January-February (DJF) season from 1950-2004. They discovered that the ERSST.v3b and MWOI-SST ONI values were highly correlated, with a correlation coefficient of 0.98. Another study by L'Heureux et al. (2017) compared the ERSST.v3b and MWOI-SST ONI values from 1979-2004 and found that the two indices were highly correlated, with a correlation coefficient of 0.93. In a third study, Hanley et al. (2003) compared the ERSST.v3b, MWOI-SST, and a third ONI index called the Tahiti-Darwin ONI. They found that the ERSST.v3b and MWOI-SST ONI values were highly correlated, with a correlation coefficient of 0.93.

Nino Region 3.4 Wind

Long term global datasets of satellite observations of wind speed and wave height provide a potentially valuable resource to study global climatology and changes in climate (Young & Donelan, 2018) . The QuikSCAT scatterometer has been operating since August 1999 to provide global mapping of ocean winds. It was shown to be accurate for wind speed of up to at least 20 m/s (Yueh et al., 2003). The following Table 3 and Figures 8 & 9 are the Monthly wind over Nino Region 3.4.

Table 3. Monthly mean Nino region 3.4 Wind based on QuickScat

Year	1	2	3	4	5	6	7	8	9	10	11	12
1999							7.93	7.02	6.34	7.29	7.27	7.44
2000	7.55	6.61	5.89	6.04	6.20	7.09	7.17	7.97	6.86	7.54	7.05	6.91
2001	6.98	6.80	5.98	6.20	6.28	7.12	7.48	7.48	6.96	6.60	7.30	7.33
2002	7.46	6.69	6.70	5.98	5.67	6.93	6.53	7.43	6.90	6.89	7.38	7.02
2003	7.47	6.67	6.25	6.14	6.58	5.64	7.43	6.69	6.44	6.40	6.45	7.72
2004	6.86	7.04	6.31	6.03	6.52	7.30	6.12	7.18	6.59	6.45	6.50	6.73
2005	7.54	6.87	6.00	6.21	5.86	6.30	7.34	6.62	6.96	7.05	6.96	7.45
2006	6.95	6.14	6.13	6.00	5.68	7.32	6.79	7.18	7.29	6.36	6.46	7.31
2007	7.27	6.72	6.40	6.05	6.15	7.21	6.54	7.36	7.65	6.72	7.51	7.42
2008	7.28	6.65	5.74	5.80	6.05	6.74	7.00	7.11	7.08	6.90	7.25	7.47
2009	6.85	6.40	5.89	5.86	6.04	6.04	7.76	6.82	7.59	5.23	6.10	

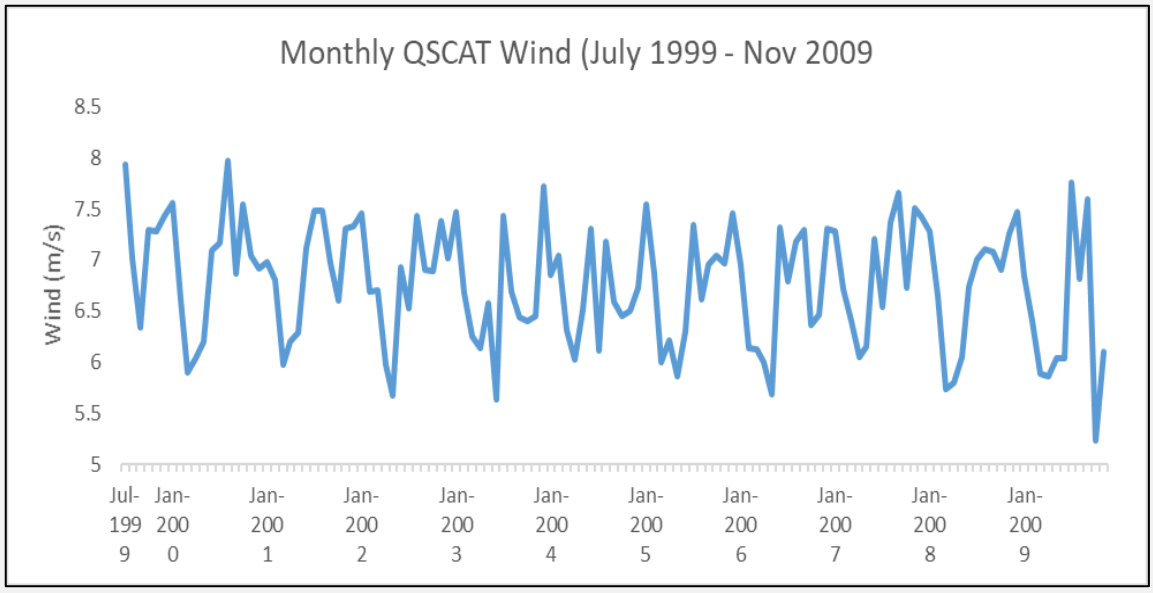

Figure 8. Monthly QSCAT Wind over Nino 3.4 region

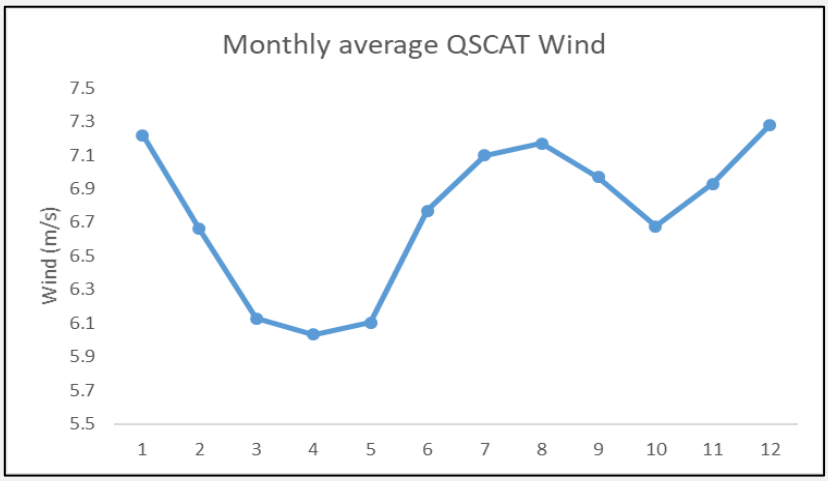

Figure 9. Monthly average QSCAT Wind over Nino 3.4 Region

The monthly mean Nino region 3.4 wind data based on QuickSCAT during the period from 1999 to 2009 would provide a record of the average wind conditions in the Nino 3.4 region over this time period, based on measurements taken by the QuikSCAT scatterometer. This data could be used for a variety of purposes, such as studying the impacts of ENSO on regional and global weather patterns, examining long-term trends in wind conditions in the Nino 3.4 region, or supporting weather forecasting and marine safety efforts.

Based on table and figures above, it is observed that the wind speed of Nino 3.4 region is range from 5.23 m/s to 7.97 m/s. Unlike Sea Surface Temperature (SST), annual average wind speed is more stable with monthly variation. The wind speed is observed high in the beginning and the end of years.

Ham et al. (2021) in their study used QuikSCAT wind data, along with other data sources, to examine the relationship between the El Nino-Southern Oscillation (ENSO) and the South American Low-Level Jet (SALLJ), a persistent wind system that plays a key role in the atmospheric circulation over South America. The authors found that the SALLJ is significantly affected by ENSO, with the strongest SALLJ winds occurring during El Nino events and the weakest winds occurring during La Nina events.

Nino Region 3.4 Sea Surface Height (SSH)

The variability and change of future sea surface height (SSH) is the center of much of the concern about the ongoing global warming. Understanding and predicting these key values, globally and regionally, involves projection and space–time integration of the numerous factors that influence SSH (Sonnewald et al., 2018).

The daily sea surface height (SSH) data of Nino Region 3.4 from January 1998 to May 2019 with 0.25° x 0.25° resolution were provided by AVISO data center of CNES (Centre National d'Etudes Spatiales) based on TOPEX/Poseidon, Jason-1, and ERS-2 data were used in this study. Those daily data were converted to monthly data by using monthly average calculation in ArcGIS Model Builder. The following table and figures are the sea surface height (SSH) of Nino region 3.4.

Based on Table 4 and Figures 10 & 11, it is observed that Sea Surface Height (SSH) over Nino 3.4 region varied from 65.8 cm to 106.8 cm. 2015 is the highest SSH with annual average of 96 cm, whereas 1999 is the lowest SSH with annual average of 71.4 cm. the SSH in the Nino Region 3.4 has been found to fluctuate on interannual to decadal timescales due to ENSO events. During El Niño events, the SSH tends to be higher than normal due to the warming of the surface water in the equatorial Pacific, while during La Niña events, the SSH tends to be lower than normal due to the cooling of the surface water.

The Sea Surface Height (SSH) in the Nino Region 3.4 demonstrates considerable interannual to decadal variability due to El Niño-Southern Oscillation (ENSO) events, as noted in studies conduct by Wang et al. (2018). During El Niño events, the SSH tends to be higher than normal due to the warming of the surface water in the equatorial Pacific, while during La Niña events, the SSH tends to be lower than normal due to the cooling of the surface water.

Table 4. Monthly mean Nino Region 3.4 Sea Surface Height (SSH)

Year	1	2	3	4	5	6	7	8	9	10	11	12
1998	89.3	80.3	76.3	72.1	67.9	66.4	67.1	67.9	70.1	69.2	69.5	70.5
1999	68.2	66.9	66.8	65.9	70.1	74.3	73.0	75.2	75.4	74.9	73.5	73.0
2000	72.6	68.9	68.5	68.7	73.3	75.7	79.3	78.1	81.2	77.7	78.6	77.9
2001	75.1	71.5	72.8	71.7	76.5	77.8	83.1	81.3	83.8	81.9	80.6	86.6
2002	82.8	80.4	76.8	76.8	82.4	81.1	89.5	88.6	94.9	98.7	90.4	92.0
2003	82.0	81.2	75.9	76.3	74.4	83.6	81.0	83.3	84.4	87.1	88.5	82.6
2004	85.0	78.1	76.0	78.8	79.4	80.1	87.1	88.5	87.6	90.4	89.5	89.4
2005	83.1	87.6	82.2	78.8	79.5	80.8	79.9	82.2	80.9	84.0	82.0	79.5
2006	75.7	74.3	75.5	75.5	79.9	80.4	86.1	87.6	87.4	91.3	92.2	85.6
2007	79.7	75.4	72.4	72.9	74.9	78.5	78.5	76.7	75.3	77.2	75.1	75.5
2008	71.5	72.0	73.0	73.5	76.0	77.9	80.3	80.6	79.4	79.6	76.8	75.5
2009	75.3	76.3	81.3	83.9	83.7	89.1	85.4	93.1	85.4	93.1	90.3	95.4
2010	87.2	89.0	81.3	78.4	73.7	73.9	74.0	71.5	71.8	72.4	73.9	72.5
2011	74.3	75.2	75.0	76.0	76.2	77.3	78.6	78.7	76.0	78.8	77.8	75.2
2012	73.3	73.0	73.0	76.2	75.9	80.0	82.4	85.1	85.3	86.1	84.4	82.4
2013	78.2	77.4	74.1	73.9	77.5	79.0	82.1	84.6	82.5	87.6	85.9	82.7
2014	81.7	85.0	89.0	84.2	85.2	84.1	84.7	88.3	87.8	90.6	91.6	89.7
2015	88.9	88.7	92.4	89.7	93.2	90.5	100.0	100.1	100.6	106.8	101.8	98.6
2016	98.1	88.8	81.6	77.7	77.1	78.9	79.8	79.8	80.6	81.9	83.8	86.7
2017	84.3	81.9	78.1	80.2	80.2	83.3	82.5	82.6	80.9	81.2	81.7	83.6
2018	80.1	82.5	81.5	84.1	87.2	88.8	88.4	91.9	93.6	95.1	95.7	91.5
2019	90.6	90.5	85.1	83.6	82.6							

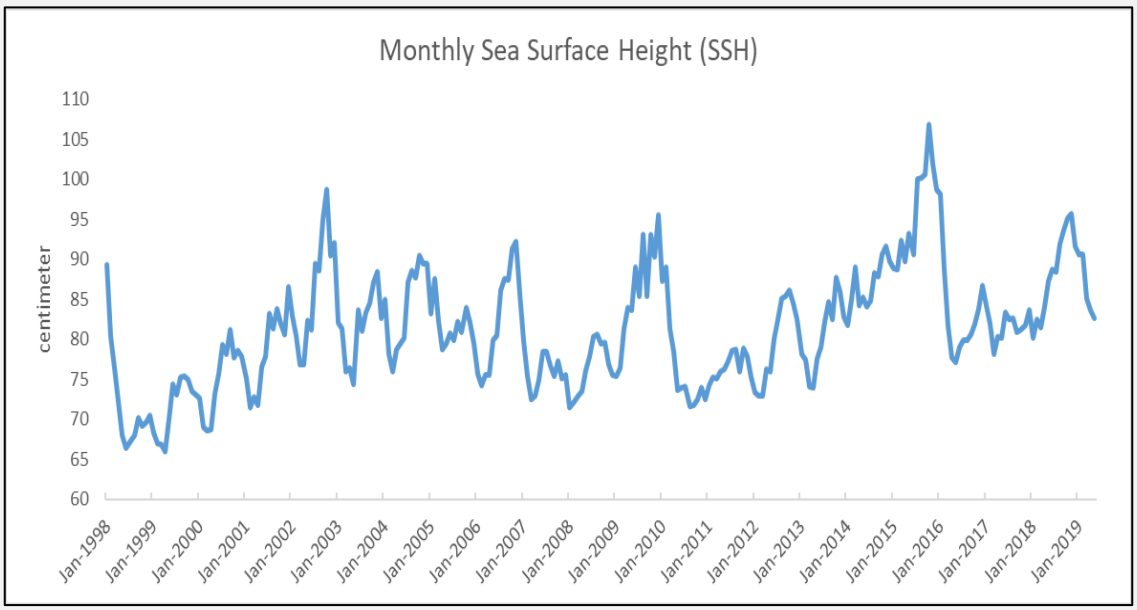

Figure 10. Monthly Sea Surface Height (SSH) over Nino 3.4 Region

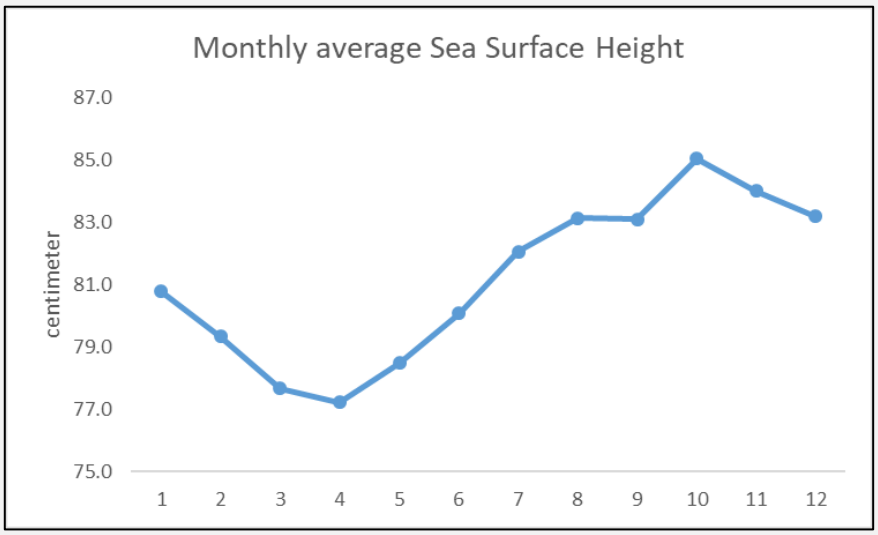

Fig 11. Monthly average SSH over Nino 3.4 Region

ENSO events can significantly affect global weather patterns, potentially leading to extreme events such as drought, floods, and hurricanes (Greenough et al., 2001). Factors influencing the SSH in the Nino Region 3.4 include atmospheric and oceanic circulation patterns, wind stress, and heat fluxes (Deser & Wallace, 1987).

Correlation of Nino Region 3.4 SST, Wind, and SSH

For further ENSO analysis, correlation analysis between SST, Wind, and SSH is needed. The following figures are the result for correlation between SST, Wind speed, and SSH over Nino 3.4 region.

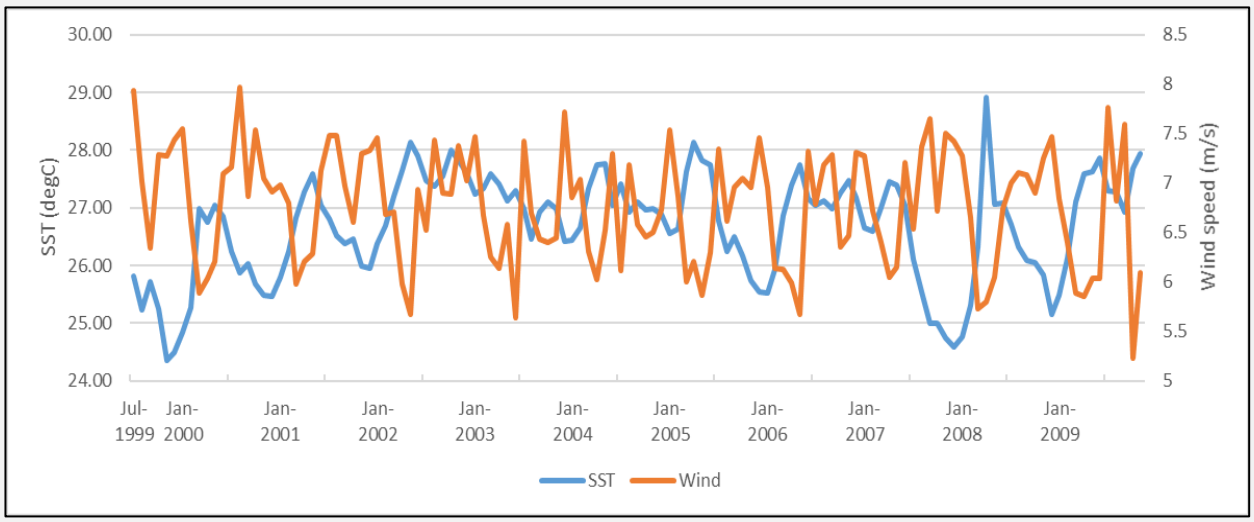

Fig 12. Monthly SST & Wind in Nino Region 3.4 (Jul 1999-Nov 2009)

Based on Figures 12-15, it is observed that Sea Surface Temperature(SST) has negative correlation with wind speed with coefficient of correlation of 0.28. Conversely, SST over Nino 3.4 region has positive correlation with Sea Surface High (SSH) with coefficient of correlation of 0.30. which mean the higher temperature, the higher Sea Surface Height.

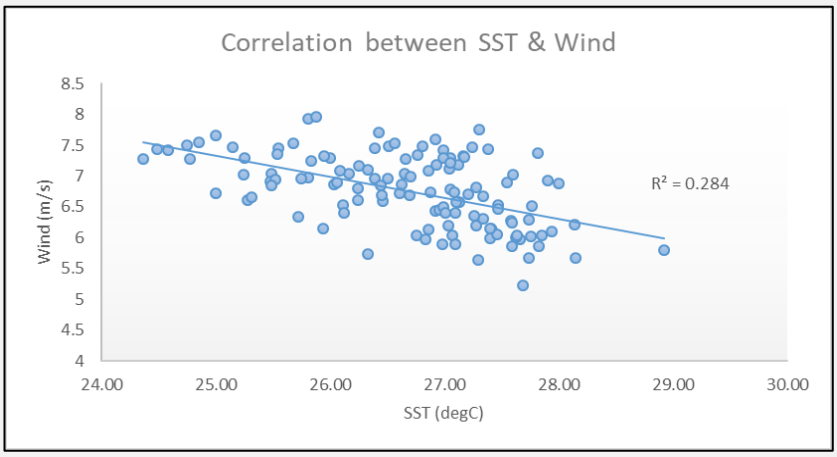

Fig 13. Correlation between SST & Wind in Nino region 3.4

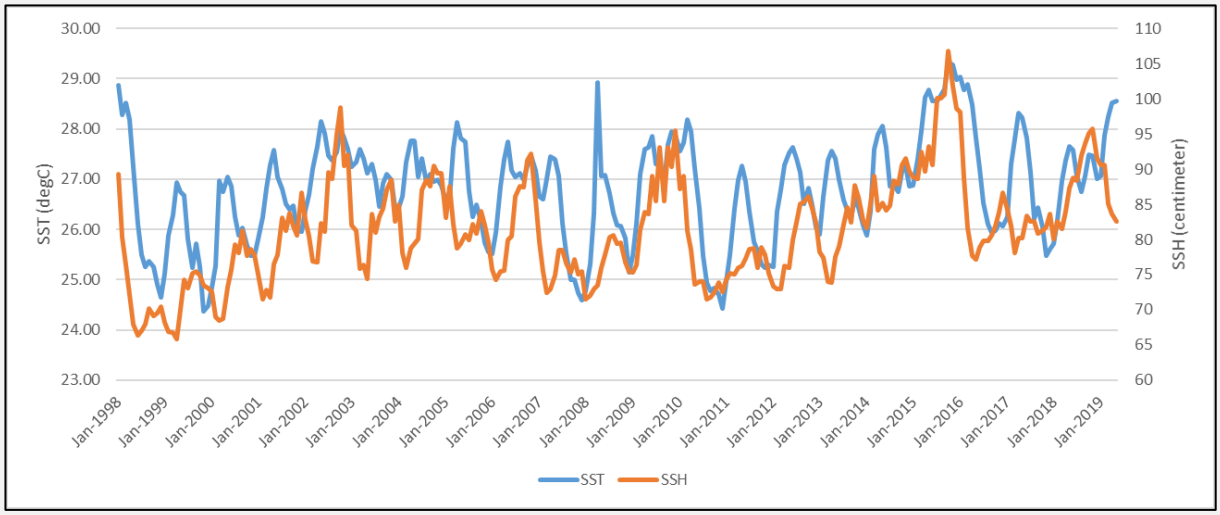

Fig 14. Monthly SST & SSH in Nino Region 3.4 (Jan 98-May 19)

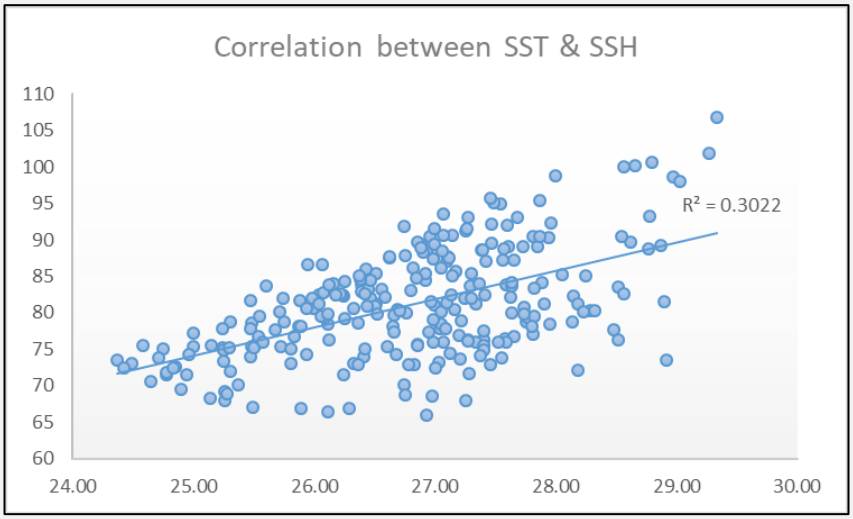

Fig 15. Correlation between SST & SSH in Nino 3.4 region

According to Wang & Wang (2016), the Nino Region 3.4 sea surface temperature (SST), wind, and sea surface height (SSH) are strongly correlated, with the wind-evaporation-SST feedback playing a key role in the development and maintenance of the Madden-Julian Oscillation (MJO). Casey & Adamec (2002) also found that the interannual variability of SST and SSH in the tropical Pacific Ocean are strongly correlated with the Nino Region 3.4 SST and influenced by the El Niño-Southern Oscillation (ENSO) and other climate phenomena such as the Pacific Decadal Oscillation (PDO). They observed a strong correlation between SST and SSH in the tropical Pacific Ocean, particularly in the Nino Region 3.4, and noted that these variables are also influenced by ENSO and other climate phenomena such as the Pacific-North American (PNA) pattern and the Atlantic Multidecadal Oscillation (AMO).

Typhoon Soudelor (2015)

Tropical cyclones, also known as typhoons (with maximum sustained 10 m wind speed greater than 32.7 m/s) in the Northwest Pacific, are an important part of the air-sea system. When typhoons pass over the ocean, the air-sea interaction leads to the exchange of heat, moisture and momentum and causes a dramatic response of the ocean (Ning et al., 2019).

The strong wind brought by typhoons causes a strong effect of entrainment, which generally decreases the sea surface temperature (SST) and increases the subsurface temperature. SST plays a major role in the energy exchange between typhoons and ocean. Therefore, it is necessary to study the SST response to typhoons. Typhoon-induced entrainment makes surface warm water sink into subsurface, leading to an increase of subsurface temperature. After typhoons, the SST gradually recovers but the thermal anomaly of subsurface warming is retained.

Typhoon Soudelor, known in the Philippines as Typhoon Hanna, was the third most intense tropical cyclone worldwide in 2015 after Hurricane Patricia and Cyclone Pam as well as the strongest tropical cyclone of the 2015 Pacific typhoon season. Soudelor had severe impacts in the Northern Mariana Islands, Taiwan, and eastern China, resulting in 40 confirmed fatalities. Lesser effects were felt in Japan, South Korea and the Philippines. The thirteenth named storm of the annual typhoon season, Soudelor formed as a tropical depression near Pohnpei on July 29. The system strengthened slowly at first before entering a period of rapid intensification on August 2. As shown in Figure 16, Typhoon Soudelor was formed on July 30 and quickly intensified from 2 August to 6 August. It reached peak intensity as a Category 5 typhoon (on the Saffir–Simpson scale) with a maximum sustained wind speed of 155 knot/h at 1800 UTC on August 3.

Microwave OI SST (MWOI SST) is used in this work to study surface response of the ocean to Typhoon Soudelor. This dataset is a merged, daily SST product with 25 km × 25 km spatial resolution, provided by Remote Sensing Systems and sponsored by National Oceanographic Partnership Program (NOPP) and the NASA Earth Science Physical Oceanography Program (http://www.remss.com/).

The cooling of the sea surface during Super Typhoon Soudelor is illustrated in Figure 17. During the typhoon's passage, there was a distinct cooling effect visible along its track, with a tendency to shift towards the right. The maximum decrease in sea surface temperature (SST) reached up to 3.43 degrees Celsius on August 6th, when Soudelor passed over an area known as a cyclone eddy region. This cooling was significantly stronger than in other areas. Figure 17 shows the relationship between SST cooling, wind speed, and sea surface height (SSH) on August 4th, 2015. From the figure, it is clear that SST cooling occurred in areas with high wind speeds and lower SSH values, specifically in cyclone eddy regions.

It is worth noting that the cooling of the sea surface during a typhoon can have significant impacts on the marine ecosystem and the global climate. Cooler sea surface temperatures can affect the distribution and behavior of marine life, as well as alter the exchange of heat and moisture between the ocean and the atmosphere. Understanding the mechanisms behind sea surface cooling during typhoons is important for predicting and mitigating their impacts on the environment.

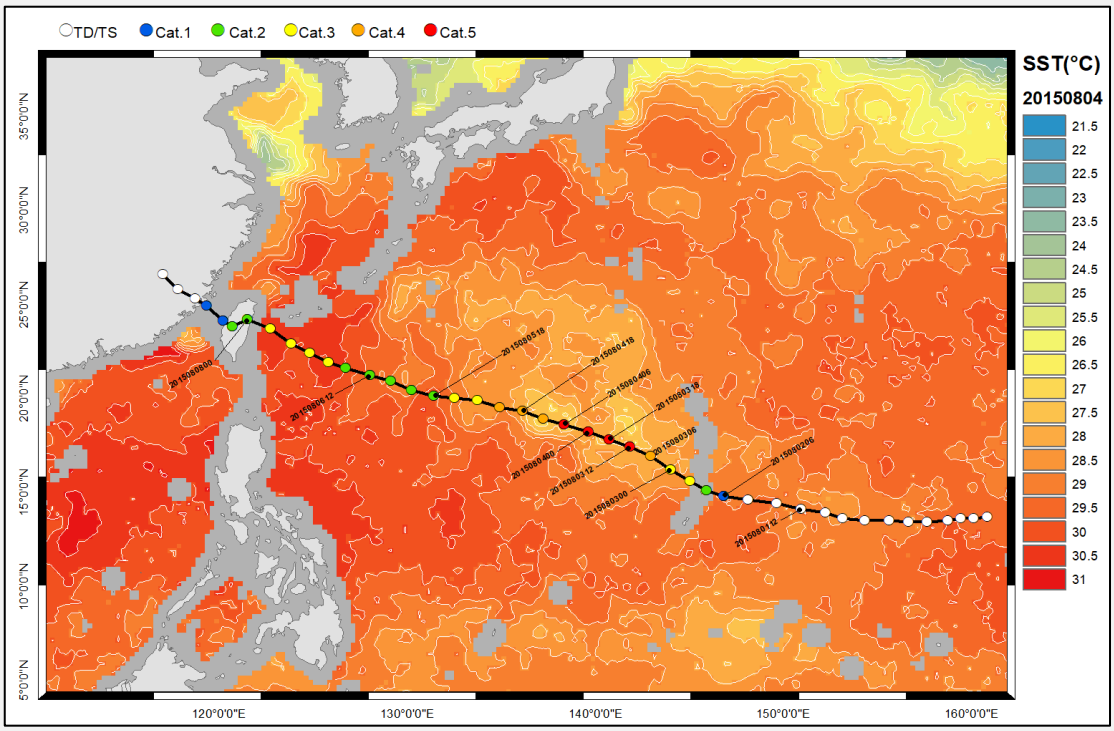

Figure 16. Track of Typhoon Soudelor with Sea Surface Temperature

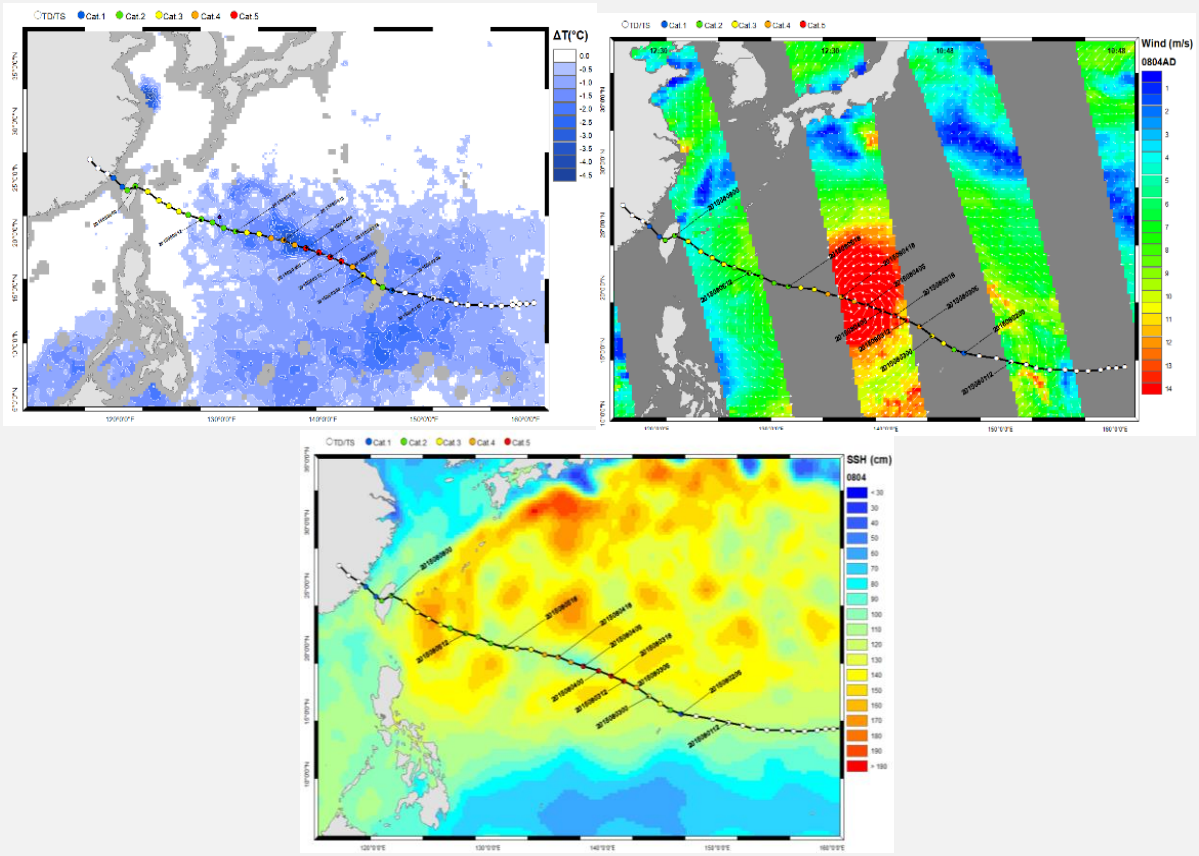

Fig 17. SST cooling, Wind speed, and SSH of Typhoon Soudelor on 4 August 2015

Correlation of El Nino and Precipitation in Specific Region

The ENSO phenomenon consists of two events, El Niño and La Niña. This phenomenon can give negative impacts to the community directly such as prolonged droughts and forest fires, and excessive rainfall which causes the flash flood. El Niño occurs when sea surface temperature (SST) in the eastern and central Pacific Ocean increase which associated to the reduction of rainfall in Indonesia whereas when La Niña occurs it shows the opposite condition (Rejeki et al., 2018).

TRMM Precipitation was used in Bandung City (Indonesia) to assess the correlation of El Nino occurrence in 2015 and precipitation in those area. Table 5 and Figure 18 show the correlation of El Nino and precipitation in Bandung City, Indonesia.

Table 5. Monthly precipitation in Bandung City, Indonesia

Month	30-year average	Year 2015
Jan	324.3	322.6
Feb	315.1	318.7
Mar	366.0	355.1
Apr	243.9	188.2
May	154.6	58.1
Jun	103.8	1.7
Jul	107.3	7.9
Aug	33.9	30.5
Sep	86.2	43.8
Oct	238.3	189.7
Nov	312.6	311.1
Dec	268.8	285.3
Total	**2554.9**	**2119.7**

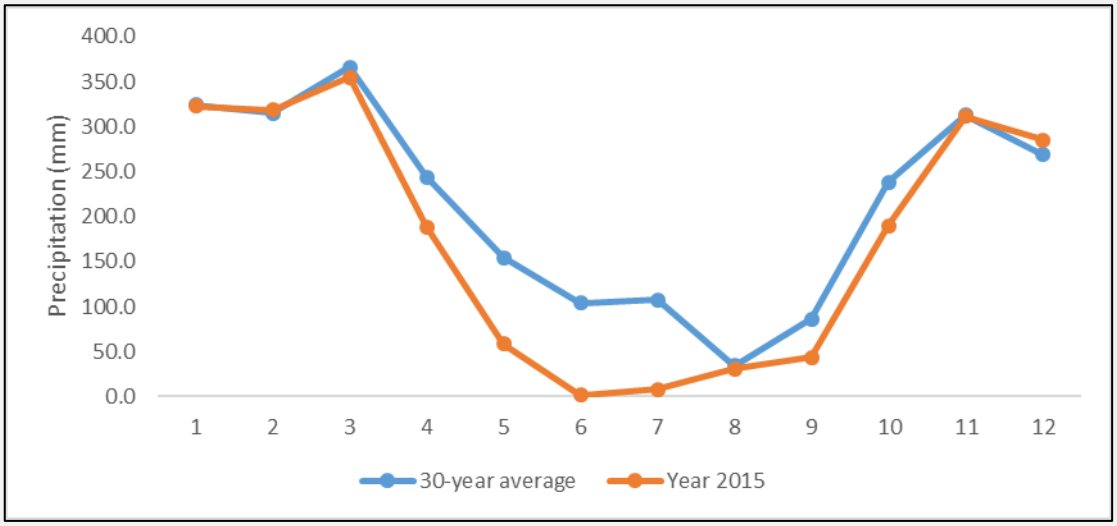

Figure 18. Comparison of 30-yr average vs 2015 monthly mean precipitation in Bandung City, Indonesia

The El Niño-Southern Oscillation (ENSO) is a natural climate phenomenon that consists of two events: El Niño and La Niña. These events can have negative impacts on communities, including prolonged droughts and forest fires, as well as excessive rainfall leading to flash floods. El Niño is characterized by an increase in sea surface temperatures in the eastern and central Pacific

Ocean, which is often associated with reduced rainfall in Indonesia. La Niña, on the other hand, is characterized by the opposite conditions.

In 2015, the Tropical Rainfall Measuring Mission (TRMM) Precipitation data was used to assess the correlation between El Niño and precipitation in Bandung City, Indonesia. The results showed that the amount of precipitation in Bandung City decreased during the dry season (May-September) of 2015, which may have been influenced by the strong El Niño event that year. This is an example of how El Niño can have direct impacts on local weather patterns and precipitation levels. It is important for communities to be aware of and prepared for the potential impacts of ENSO events in order to mitigate their negative effects.

CONCLUSION

The results of the study showed that the MWOI-SST Ocean Nino Index had a very strong correlation with ERSST.v5, with a coefficient of correlation of 0.92 and an RMSE of 0.36°C. The wind speed in the Nino 3.4 region ranged from 5.23 m/s to 7.97 m/s, and the annual average wind speed was found to be more stable with monthly variations. The wind speed was observed to be high at the beginning and end of the year. The SSH in the Nino 3.4 region varied from 65.8 cm to 106.8 cm, with 2015 being the year with the highest SSH (96 cm) and 1999 being the year with the lowest SSH (71.4 cm).

The study also found that there was a negative correlation between SST and wind speed, with a coefficient of correlation of 0.28, and a positive correlation between SST and SSH, with a coefficient of correlation of 0.30. This means that higher temperatures are associated with higher SSH values. During the passage of Typhoon Soudelor, a cool trail with a rightward bias was observed along its track. The researchers also found that the decreasing precipitation in Bandung City may have been influenced by the strong El Nino event in 2015.

REFERENCES

Banholzer, S., & Donner, S. (2014). The influence of different El Niño types on global average temperature. *Geophysical Research Letters*, *41*(6), 2093-2099. https://doi.org/10.1002/2014GL059520

Casey, K. S., & Adamec, D. (2002). Sea surface temperature and sea surface height variability in the North Pacific Ocean from 1993 to 1999. *Journal of Geophysical Research: Oceans*, *107*(C8), 14-1. https://doi.org/10.1029/2001JC001060

Church, J. A., & White, N. J. (2006). A 20th century acceleration in global sea-level rise. *Geophysical research letters*, *33*(1). https://doi.org/10.1029/2005GL024826

Deliège, A., & Nicolay, S. (2017). Analysis and indications on long-term forecasting of the oceanic Niño index with wavelet-induced components. *Pure and Applied Geophysics*, *174*(4), 1815-1826. https://doi.org/10.1007/s00024-017-1491-4

Deser, C., & Wallace, J. M. (1987). El Niño events and their relation to the Southern Oscillation: 1925–1986. *Journal of Geophysical Research: Oceans*, *92*(C13), 14189-14196. https://doi.org/10.1029/JC092iC13p14189

Glantz, M. H., & Ramirez, I. J. (2020). Reviewing the Oceanic Niño Index (ONI) to enhance societal readiness for El Niño's impacts. *International Journal of Disaster Risk Science*, *11*(3), 394-403. https://doi.org/10.1007/s13753-020-00275-w

Greenough, G., McGeehin, M., Bernard, S. M., Trtanj, J., Riad, J., & Engelberg, D. (2001). The potential impacts of climate variability and change on health impacts of extreme weather events in the United States. *Environmental health perspectives*, *109*(suppl 2), 191-198. https://doi.org/10.1289/ehp.109-1240666

Ham, Y. G., Lee, H. J., Jo, H. S., Lee, S. G., Cai, W., & Rodrigues, R. R. (2021). Inter-Basin Interaction Between Variability in the South Atlantic Ocean and the El Niño/Southern Oscillation. *Geophysical Research Letters*, *48*(15), e2021GL093338. https://doi.org/10.1029/2021GL093338

Hanley, D. E., Bourassa, M. A., O'Brien, J. J., Smith, S. R., & Spade, E. R. (2003). A quantitative evaluation of ENSO indices. *Journal of Climate*, *16*(8), 1249-1258. https://doi.org/10.1175/1520-0442(2003)16%3C1249:AQEOEI%3E2.0.CO;2

Hartmann, D. L. (2015). Pacific sea surface temperature and the winter of 2014. *Geophysical Research Letters, 42*(6), 1894-1902. https://doi.org/10.1002/2015GL063083

Hayashi, M., Jin, F. F., & Stuecker, M. F. (2020). Dynamics for El Niño-La Niña asymmetry constrain equatorial-Pacific warming pattern. *Nature communications, 11*(1), 1-10. https://doi.org/10.1038/s41467-020-17983-y

Holton, J. R., & Hakim, G. J. (2013). The General Circulation. in *An Introduction to Dynamic Meteorology*. https://doi.org/10.1016/b978-0-12-384866-6.00010-6

Jorgensen, D. (2016). The garden and beyond: The dry season, the Ok Tedi shutdown, and the footprint of the 2015 El Niño drought. *Oceania*, *86*(1), 25-39. https://doi.org/10.1002/ocea.5121

Kovats, R. S. (2000). El Niño and human health. *Bulletin of the World Health Organization, 78*, 1127-1135.

L'Heureux, M. L., Takahashi, K., Watkins, A. B., Barnston, A. G., Becker, E. J., Di Liberto, T. E., Gamble, F., Gottschalck, J., Halpert, M., Huang, B., Mosquera-Vásquez, K., & Wittenberg, A. T. (2017). Observing and predicting the 2015/16 El Niño. *Bulletin of the American Meteorological Society*, *98*(7), 1363-1382. https://doi.org/10.1175/BAMS-D-16-0009.1

L'Heureux, M. L., & Wallace, J. M. (2006). Comparisons of ENSO indices based on in situ and satellite SST observations. Journal of Climate, 19(17), 4529-4541.

Li, Y., & Han, W. (2015). Decadal sea level variations in the Indian Ocean investigated with HYCOM: Roles of climate modes, ocean internal variability, and stochastic wind forcing. *Journal of Climate*, *28*(23), 9143-9165. https://doi.org/10.1175/JCLI-D-15-0252.1

Lyon, B., & Camargo, S. J. (2009). The seasonally-varying influence of ENSO on rainfall and tropical cyclone activity in the Philippines. Climate Dynamics, 32(1), 125-141. https://doi.org/10.1007/s00382-008-0380-z

Merchant, C. J., Minnett, P. J., Beggs, H., Corlett, G. K., Gentemann, C., Harris, A. R., Hoyer, J., & Maturi, E. (2019). Global Sea Surface Temperature. In *Taking the Temperature of the Earth*. https://doi.org/10.1016/b978-0-12-814458-9.00002-2

Nachshon, U., Dragila, M., & Weisbrod, N. (2012). From atmospheric winds to fracture ventilation: Cause and effect. Journal of Geophysical Research: Biogeosciences, 117(G2). https://doi.org/10.1029/2011JG001898

Ning, J., Xu, Q., Zhang, H., Wang, T., &Fan, K. (2019). Impact of cyclonic ocean eddies on upper ocean thermodynamic response to Typhoon Soudelor. *Remote Sensing, 11*(8). https://doi.org/10.3390/rs11080945

O'Carroll, A. G., Armstrong, E. M., Beggs, H. M., Bouali, M., Casey, K. S., Corlett, G. K., Dash, P., Donlon, C.J., Gentemann, C.L., Høyer, J.L., & Wimmer, W. (2019). Observational needs of sea surface temperature. *Frontiers in Marine Science*, *6*, 420. https://doi.org/10.3389/fmars.2019.00420

Philander, S. G. (1989). El Niño, La Niña, and the southern oscillation. *International geophysics series*, *46*, X-289.

Prasetyo, Y., & Nabilah, F. (2017). Pattern Analysis of El Nino and la Nina Phenomenon Based on Sea Surface Temperature (SST) and Rainfall Intensity using Oceanic Nino Index (ONI) in West Java Area. *IOP Conference Series: Earth and Environmental Science*, *98*(1). https://doi.org/10.1088/1755-1315/98/1/012041

Rejeki, H. A., Kunarso, K., & Munasik, M. (2018). Interannual variability of sea surface height difference between western Pacific Ocean and eastern Indian Ocean and its effect to geostrophic current in Lombok Strait. *IOP Conference Series: Earth and Environmental Science, 162*(1). https://doi.org/10.1088/1755-1315/162/1/012016

Rodríguez-Morata, C., Díaz, H. F., Ballesteros-Canovas, J. A., Rohrer, M., & Stoffel, M. (2019). The anomalous 2017 coastal El Niño event in Peru. *Climate Dynamics, 52*(9), 5605-5622. https://doi.org/10.1007/s00382-018-4466-y

Shabbar, A. (2006). The impact of El Niño-southern oscillation on the Canadian climate. *Advances in Geosciences, 6*, 149-153. https://doi.org/10.5194/adgeo-6-149-2006

Sonnewald, M., Wunsch, C., &Heimbach, P. (2018). Linear predictability: A sea surface height case study. *Journal of Climate*, *31*(7), 2599–2611. https://doi.org/10.1175/JCLI-D-17-0142.1

Wang, C., & Fiedler, P. C. (2006). ENSO variability and the eastern tropical Pacific: A review. *Progress in oceanography*, *69*(2-4), 239-266. https://doi.org/10.1016/j.pocean.2006.03.004

Wang, C., Deser, C., Yu, J. Y., DiNezio, P., & Clement, A. (2017). El Niño and southern oscillation (ENSO): a review. *Coral reefs of the eastern tropical Pacific*, 85-106. https://doi.org/10.1007/978-94-017-7499-4_4

Wang, F., Li, Y., & Wang, J. (2016). Intraseasonal variability of the surface zonal currents in the western tropical Pacific Ocean: Characteristics and mechanisms. *Journal of Physical Oceanography*, *46*(12), 3639-3660. https://doi.org/10.1175/JPO-D-16-0033.1

Wang, H., Liu, K., Wang, A., Feng, J., Fan, W., Liu, Q., Xu, Y., & Zhang, Z. (2018). Regional characteristics of the effects of the El Niño-Southern Oscillation on the sea level in the China Sea. *Ocean Dynamics*, *68*(4), 485-495. https://doi.org/10.1007/s10236-018-1144-x

Wu, Z., Wang, B., Li, J., & Jin, F. F. (2009). An empirical seasonal prediction model of the East Asian summer monsoon using ENSO and NAO. *Journal of Geophysical Research: Atmospheres*, *114*(D18). https://doi.org/10.1029/2009JD011733

Young, I. R., & Donelan, M. A. (2018). On the determination of global ocean wind and wave climate from satellite observations. *Remote Sensing of Environment*, *215*, 228–241. https://doi.org/10.1016/j.rse.2018.06.006

Yueh, S. H., Stiles, B. W., & Liu, W. T. (2003). QuikSCAT wind retrievals for tropical cyclones. *IEEE Transactions on Geoscience and Remote Sensing*, *41*(11), 2616-2628. https://doi.org/10.1109/TGRS.2003.814913

Zhuang, W., Xie, S. P., Wang, D., Taguchi, B., Aiki, H., & Sasaki, H. (2010). Intraseasonal variability in sea surface height over the South China Sea. *Journal of Geophysical Research: Oceans, 115*(C4). https://doi.org/10.1029/2009JC005647